NASA TECHNICAL MEMORANDUM

NASA TM X-71573

NASA TM X-71573

EFFECT OF POLLUTANT GASES ON OZONE PRODUCTION BY SIMULATED SOLAR RADIATION

by E. L. Wong and David A. Bittker
Lewis Research Center
Cleveland, Ohio 44135

TECHNICAL PAPER proposed for presentation at the
Second International Conference on the Environmental
Impact of Aerospace Operations in the High Atmosphere
sponsored by the American Meteorological Society
and the American Institute of Aeronautics and Astronautics
San Diego, California, July 8-10, 1974

EFFECT OF POLLUTANT GASES ON OZONE PRODUCTION BY SIMULATED SOLAR RADIATION

by E. L. Wong and David A. Bittker

Lewis Research Center

E-8013

INTRODUCTION

The present investigation provides some information related to the problem of ozone destruction by nitric oxide, NO, emission from high flying vehicles. According to Johnston (1971) and Westenberg (1972), NO emission could catalytically destroy ozone, O_3, in the upper atmosphere to such an extent that additional ultraviolet, u.v., radiation would reach the earth with possible harmful effects.

F. E. Belles of this Center suggested that if Johnston and Westenberg had included certain photochemical smog reactions in their NO-O_3 destruction scheme, NO destruction of O_3 might be reduced. Rapid NO conversion to nitrogen dioxide, NO_2, followed by production of O_3, has been observed in smog chamber experiments and Los Angeles smog (Leighton (1961)). This rapid NO conversion process to NO_2 followed by O_3 production is now believed to be a chain reaction involving unsaturated hydrocarbon and/or carbon monoxide, CO, oxidation (Leighton (1961), Heicklen et al. (1969), Westberg and Cohen (1971)). Thus, if engine exhausts have insufficient amounts of unsaturated hydrocarbon and CO to counteract the destruction of O_3 by the NO emitted, additional appropriate amounts of unsaturated hydrocarbon and/or CO could be added to engine exhaust gases.

Based on Belles' recommendation, experiments were conducted using simulated solar radiation in a chamber with controlled atmosphere. Pressure was near 1 atmosphere in these tests. Tests were made to evaluate NO destruction of O_3 in the chamber and to determine if addition of CO and H_2O could reduce NO destruction of O_3. In conjunction with these experiments, the General Chemical Kinetics Program (Bittker and

Scullin (1972)) developed at the Lewis Research Center was modified and extended to permit a detailed kinetics data analysis.

CHEMICAL BACKGROUND

When pure air is irradiated with ultraviolet light, the formation of O_3 is controlled chemically by the Chapman mechanism, as represented by the following reactions:

$$h\nu + O_2 \xrightarrow{J_1} O + O \qquad \text{(I)}$$

$$O + O_2 + M \xrightarrow{k_2} O_3 + M \qquad \text{(II)}$$

$$h\nu + O_3 \xrightarrow{J_3} O + O_2 \qquad \text{(III)}$$

$$O + O_3 \xrightarrow{k_4} 2\,O_2 \qquad \text{(IV)}$$

The recombination reaction $O + O + M \rightarrow O_2 + M$ also occurs, but is of negligible importance at atmospheric and stratospheric conditions. In this discussion we neglect the formation of excited state species in the photolysis reactions. If it is assumed that oxygen atom concentration rapidly reaches a steady state value, then one can derive a differential equation for O_3 production in which all terms containing J_3 are negligibly small. This equation can be integrated to give the following expression

$$[O_3] = \frac{\nu_2}{k_4}\left[1 - e^{-\left(\frac{k_4 J_1 t}{k_2[M]} + \frac{k_4[O_3]}{2\nu_2}\right)}\right] \qquad (1)$$

where

t = reaction time

$[O_3]$ = molar O_3 concentration

$[M]$ = total molar concentration

$\nu_2 = k_2[O_2][M]$

In the expression e^{-x}, the exponent x is smaller than 0.1 for reaction times up to about 1000 hours, so that the expansion

$$e^{-x} \cong 1 - x$$

can be used. When this is done, the above equation becomes

$$[O_3] = 2J_1[O_2]t \tag{2}$$

Therefore, when pure air is irradiated, O_3 concentration should rise linearly for a long time. The rate of rise is determined only by the rate of photolysis of O_2 to form oxygen atoms.

When dry air is irradiated in the presence of oxides of nitrogen, the following additional reactions occur which tend to destroy O_3:

$$NO + O_3 \xrightarrow{k_5} NO_2 + O_2 \tag{V}$$

$$h\nu + NO_2 \xrightarrow{J_6} NO + O \tag{VI}$$

$$O + NO_2 \xrightarrow{k_7} NO + O_2 \tag{VII}$$

$$NO_2 + O_3 \xrightarrow{k_8} NO_3 + O_2 \tag{VIII}$$

$$2NO + O_2 \xrightarrow{k_9} 2NO_2 \qquad \text{(IX)}$$

$$NO + O + M \xrightarrow{k_{10}} NO_2 + M \qquad \text{(X)}$$

$$h\nu + NO_3 \xrightarrow{J_{11}} NO + O_2 \qquad \text{(XI)}$$

Johnston (1971) and Westenberg (1972) present steady-state mathematical analyses with the above mechanism. They show that the final O_3 concentration level is indeed much lower than it is when oxides of nitrogen are not present. However, in assessing the effect of pollutants injected into the atmosphere, it is necessary to obtain the time variation of O_3 concentration from the instant of injection. To obtain such concentration profiles the chemical mechanism must be numerically integrated. To perform this kind of computation, a general chemical kinetics program was developed several years ago at the Lewis Research Center (Bittker and Scullin (1972)). It has recently been expanded and improved to allow the inclusion of more types of reactions, including photochemistry and to make the integration method more efficient. This program has been used extensively in the present work to analyze and interpret the experimental results.

As mentioned previously the presence of H_2O and CO in jet engine exhaust gases gives rise to a series of reactions which may counteract the destruction of ozone (Heicklen et al. (1969)).

$$CO + OH \xrightarrow{k_{12}} CO_2 + H \qquad \text{(XII)}$$

$$H + O_2 + M \xrightarrow{k_{13}} HO_2 + M \qquad \text{(XIII)}$$

$$NO + HO_2 \xrightarrow{k_{14}} NO_2 + OH \qquad \text{(XIV)}$$

$$H + NO_2 \xrightarrow{k_{15}} NO + OH \qquad \text{(XV)}$$

Reactions XII through XIV are quite fast and provide a strong competitive path for the conversion of NO to NO_2 without the destruction of O_3. Reaction XV, which could regenerate NO, was found to be unimportant under our experimental conditions. One must also consider the possible destruction of O_3 in the presence of H_2O alone, according to the chain mechanism:

$$OH + O_3 \xrightarrow{k_{16}} HO_2 + O_2 \qquad \text{(XVI)}$$

$$HO_2 + O_3 \xrightarrow{k_{17}} OH + 2\ O_2 \qquad \text{(XVII)}$$

The net effect of these last reactions is the conversion of two molecules of O_3 to three molecules of oxygen. In fact, H_2O and not NO was originally thought to be the main destroyer of O_3 in engine exhaust gases (Kellogg (1970)). The most recent information on the values of k_{16} and k_{17} indicates that they are much smaller than originally estimated (Garvin and Hampson (1974) and DeMore (1973)). The destruction of O_3 by NO is now considered much more important than its destruction by the water mechanism. Nevertheless the mechanism of reactions XVI and XVII cannot be ignored when studying atmospheric chemistry. The effect of water on O_3 production has been studied briefly in the present work.

The formation of nitric and nitrous acids, HNO_3 and HNO_2, has been suggested by many people as a means of removing NO from the stratosphere and thus reducing its destructive effect on ozone (Crutzen (1972), DeMore (1973), Dütsch (1972)). The possible formation of these species in the gas phase during the present work was checked by theoretical computations using these additional reactions:

$$NO + OH + M \xrightarrow{k_{18}} HNO_2 + M \qquad \text{(XVIII)}$$

$$OH + HNO_2 \xrightarrow{k_{19}} H_2O + NO_2 \qquad \text{(XIX)}$$

$$NO_2 + OH + M \xrightarrow{k_{20}} HNO_3 + M \qquad \text{(XX)}$$

$$OH + HNO_3 \xrightarrow{k_{21}} H_2O + NO_3 \qquad \text{(XXI)}$$

APPARATUS AND MATERIALS

The main apparatus for this experimental work consists of a chamber, a solar simulator, and instrumentation for monitoring O_3 and NO_x (NO and NO_2) concentrations.

Reaction Chamber

An existing chamber at this Center was modified to permit addition of pollutant gases and gas sampling (Fig. 1). The chamber has a volume of about 650 liters (23 cu ft) with approximate dimensions of 82 cm ($32\frac{1}{4}$ in.) inside diameter, and length of 122 cm (48 in.). Radiation enters the chamber through a 30.5 cm (12 in.) diameter quartz window at one end. In front of this window is a water cooled shutter so that radiation can be turned "on" or "off" instantly. This chamber can be evacuated to the low 10^{-6} torr range using a 30.5 cm (12 in. dia.) oil diffusion pump fitted with a liquid nitrogen cold trap. The inside chamber surface is stainless steel. The radiation, after passage through the 30.5 cm window, is a slightly diverging beam inside the chamber, as shown in Fig. 1. At the opposite end of the chamber the radiation describes a light circle of about 40.6 cm (16 in.) in diameter. This indicates that about one-fifth of the effective chamber volume was exposed

to the radiation. Two Teflon sampling probes were positioned to sample gas in the center of the light beam in the chamber (Fig. 1).

Solar Simulator

Simulated solar radiation was provided by a commercial solar simulator. With the apparatus shown in Fig. 1, the amount of O_3 produced in the chamber when dry clean air is irradiated, depends to a large extent on the type of xenon arc lamp used. Three types of 4.2 kW xenon high pressure arc lamps - I. T. T., Ushio, and Osram - compatible with our solar simulator were tested. The peak O_3 production in pphm was as follows:

	pphm
I. T. T.	20-30
Ushio	40-60
Osram	120-140

Due to its much higher O_3 production, an Osram lamp was used throughout this study. According to the manufacturer such lamps will provide u.v. radiation beginning at about 200 nm. In the visible range its radiation is comparable to that emitted by the sun. Ultraviolet transmission through the quartz window was measured only as low as 250 nm, but it is possible that some radiation as low as 200 nm is also present in the transmitted light.

Analytical Instruments

For this work two types of commercially available chemiluminescence analyzers were used to monitor O_3 and NO_x ($NO + NO_2$). Both instruments can only be used to sample at or near atmospheric pressure condition (low pressure limit ~700 torr). Because of this limitation the work reported here was obtained for the near atmospheric pressure condition only.

Test Gases

Clean dry air used in the irradiation experiment was commercially available tanked ultrapure clean ("UPC") air. This "UPC" air generally has the following typical stated analysis for contaminants in ppm by volume:

CO_2	0.5	N_2O (nitrous oxide)	0.1
CO	1.0	Total hydrocarbon	0.1
CH_4 (methane)	1.0	H_2O	≤ 1.0

Desired amounts of H_2O were added to "UPC" air by saturating the air with distilled H_2O at some pre-selected low temperature just prior to its entry into the chamber.

Two other tanked gases were used. A mixture of NO (18 ppm) in nitrogen was used to calibrate the NO_x analyzer and to introduce NO gas into the chamber. CO had a stated purity of 99.5 percent, and mass spectrometer analysis indicated that the 0.5 percent impurity in CO was mainly CO_2.

EXPERIMENTAL RESULTS

Evaluation of Apparatus for Ozone Production

For the O_3 production tests the tank is first pumped to the low 10^{-6} torr range for about a 20 hour period. Then "UPC" air is used to fill the tank to near atmospheric pressure. At time "zero," irradiation of this air is begun by removal of the shutter over the quartz window. The O_3 concentration in the tank is monitored as a function of time. Two O_3 production tests were made in succession on the same day, and these are shown in Fig. 2 where O_3 concentration in pphm is plotted against irradiation time in minutes. During these tests the chamber surface had not been exposed to any pollutant gases such as CO, NO_x, or H_2O. For the two runs it is interesting to note that O_3 production for the second run was much more regular. Results of these and other runs suggest that a wall conditioning process was occurring. After this conditioning

process, O_3 production rate was less erratic. In the second run, peak steady state O_3 concentration was about 115 pphm in an irradiation time of about 40 minutes. Also on the same figure is shown the ozone decay (dark circled data) when irradiation is stopped. For the two runs the decay was an exponential one. Decay rates for the first and second run were about 0.011 min^{-1} and 0.015 min^{-1}, respectively. These results indicate that the O_3 decay may not be due entirely to wall reaction alone, otherwise one would expect the decay rate for the second run (after wall conditioning) would be less than that for the first run.

Effect of Addition of NO to "UPC" Air on O_3 Production

The effect of adding varying amounts of NO to "UPC" air on O_3 production is shown in Figs. 3, 4, and 5. For purpose of comparison, an O_3 production reference curve for air alone is shown in the three figures. This reference curve is an average of some O_3 production data for air alone obtained just before and after these tests involving addition of NO were made. Figure 3 shows that when air containing an initial concentration of 30 pphm NO (as measured by the NO_x analyzer), is irradiated, the O_3 production is affected only slightly. Unfortunately, the NO_x analyzer during these three runs could measure oxides of nitrogen as total NO_x only. It is interesting to note that the total NO_x decreased almost linearly with time.

Figure 4 shows that when the initial NO is about 65 pphm, the NO inhibiting effect on O_3 production is increased as compared to the results with 30 pphm NO (Fig. 3). The O_3 production delay time is about 20 minutes. This delay time is defined as being the time duration from time zero to a time at which the O_3 production rate is about 0.2 pphm per minute. The interesting thing here is that this inhibiting effect is only temporary, since the total NO_x in the chamber is again decreasing almost linearly with time.

When the initial NO is 128 pphm (Fig. 5), the NO inhibiting effect is increased to the extent that the delay time is now about 80 minutes. Again the total NO_x decreases with time, but in a more nonlinear manner.

A fourth run, in which the NO was about 60 pphm, was made when the NO_x analyzer was fully operational. These results are shown in Fig. 6. The O_3 reference curve for "UPC" air alone was obtained a day before this run. These results agree reasonably well with those shown in Fig. 4, in which the added NO was about 65 pphm. The NO_x measurements shown in Fig. 6 can now explain partly why the NO inhibiting effect is only temporary. Measurements of NO and NO_2 indicate that NO is rapidly consumed, or converted to NO_2 (by reaction with O_3), and that no NO was regenerated. This suggests that for our experimental condition, both reaction VI ($NO_2 + h\nu \rightarrow NO + O$) and reaction VII ($NO_2 + O \rightarrow NO + O_2$) were inoperative in recycling NO. The gradual decrease in NO_2 may indicate further reactions involving NO_2 to form N_2O_5, dinitrogen pentoxide. This N_2O_5 can, perhaps, be removed by a heterogeneous reaction with trace moisture on the chamber walls to form HNO_3, nitric acid (Gay and Bufalini (1971)). These reactions will be discussed later in more detail.

Figure 7 is a summary curve showing the effect of varying amounts of initial NO on O_3 production. These experiments indicate that the observed inhibiting effect of NO is due mostly to gas phase chemical reactions.

Effect of Addition of CO, NO, and H_2O to "UPC" Air on O_3 Production

The next series of tests consisted of determining the effect on O_3 production of addition of some initial CO and H_2O to "UPC" air containing some NO. Prior to these runs involving CO and H_2O addition, a run was made to determine the effect on O_3 production of adding initially 76 pphm NO and about 1200 ppm H_2O to air. This result is shown in Fig. 8. On this same figure is another reference curve for air alone, obtained a day prior to the air + NO + H_2O run. As expected, when some NO is present, a delay in O_3 production is observed. Unexpectedly, the O_3 production eventually exceeds that for air alone temporarily. The delay time is about 25 minutes, which is about the same

as that when the initial NO was 60 or 65 pphm in dry air (Figs. 4 and 6).

The effect of initial addition of 50 ppm CO to air containing about 75 pphm NO and about 1200 ppm H_2O is shown in Fig. 9. Two comparison curves are presented, one for "UPC" air alone and the other for "UPC" air containing some added NO and H_2O. The addition of CO results in a slight decrease in O_3 production delay time to about 21 minutes versus 25 minutes in the absence of CO. No NO_x measurements were obtained for this run due to a breakdown in the NO_x analyzer.

The effect of adding initially 100 ppm CO to "UPC" air containing 60 pphm NO and about 1200 ppm H_2O is shown in Fig. 10. For this run the NO_x analyzer was fully operational, and NO and NO_2 measurements were made. These results showed that when more CO is added, the delay time is now reduced to about 9 minutes versus 21 minutes when the added CO was 50 ppm. In addition, the peak O_3 production was increased to about 162 pphm. This additional O_3 production may be attributed to the action of photosmog type reactions occurring in the reaction chamber. NO_x measurements showed that the NO_x decay is now an exponential one, whereas in the absence of CO, the NO_x decay was more linear and slower (see Figs. 3 to 6). Peak NO_2 formation was reached in about 25 minutes versus 50 minutes when no CO was present (Fig. 6). Again no NO was regenerated just as in the work involving addition of NO alone.

When the CO concentration was increased to about 220 ppm, the effect on O_3 production is shown in Fig. 11. Delay time is now further reduced to about 1 minute and O_3 production of about 172 pphm was reached. The NO_x measurements indicated that both NO and NO_x decays were accelerated, and peak NO_2 concentration occurred in about 14 minutes instead of 25 minutes, when 100 ppm CO was added. It was observed again that no NO was regenerated.

Figure 12 is a summary plot showing the effect of additions of varying amounts of CO to counteract the NO inhibiting effect on O_3 production. These experimental results indicate that CO and H_2O addition can counteract the NO destruction of O_3 and result in higher O_3 concentration in the chamber.

COMPARISON OF EXPERIMENTAL AND THEORETICAL RESULTS

Results With Pure Air

The steady-state analysis with the simple Chapman mechanism (reactions I-IV) mentioned previously shows that these reactions alone cannot account for the observed leveling off of the O_3 concentration in the chamber. An additional destruction reaction for O_3 has to be used in the chemical mechanism. This single reaction is used to represent a destruction process which may be a combination of surface and gas phase processes. For computations with our general chemical kinetics program, both simple first order and second order kinetics were used for the additional destruction reaction to see if either assumption would be more consistent with the experimental results. For all computations air was assumed to be 79.05 mole percent N_2 and 20.95 percent O_2.

The exact intensity versus wavelength distribution of our solar simulator light source was not known below 250 nm. Thus, none of the photochemical rate constants could be computed exactly. Therefore, for all computations, reasonable literature values were used at the start. When necessary they were changed within reasonable limits to give agreement between experimental and computed results. The steady-state analysis with the Chapman mechanism shows that reaction I, the oxygen photolysis, completely controls the rate of formation of O_3 in the early stages of the reaction. Several preliminary computations established that any computed O_3 concentration profile is controlled only by two rate constants. These are J_1, for the oxygen photolysis, and the rate constant for the assumed extra O_3 destruction reaction in addition to reactions III and IV. These last two reactions can in no way account for the leveling off of the O_3 concentration in our experiment. A series of computations was done with two different destruction reactions, using each separately. The overall destruction reaction used is either

$$O_3 \xrightarrow{k_{D_1}} (3/2)O_2 \qquad (D_1)$$

or

$$2\,O_3 \xrightarrow{k_{D_2}} 3\,O_2 \qquad (D_2)$$

In performing the computations, the value of J_1 was chosen to match the initial slope of the O_3 concentration versus time curve. Then the value of k_{D_1} or k_{D_2} was chosen to agree with the final portion of the concentration profile. In this analysis a computed curve is chosen to match experimental data in a semiquantitative way. It is a curve which, in the authors' judgement, closely represents the trend and magnitudes of the experimental data. This technique calibrates our system and these rate constants can then be used to analyze the experimental results in the presence of various amounts of pollutants. Inasmuch as there is a small effect of diffusion of ozone from the lighted volume of the reaction chamber to the wall, the rate constants found in this procedure also include any diffusion effects.

Computations were also made to match the experimentally observed ozone decay in our chamber. This was done to obtain preliminary values of k_{D_1} and k_{D_2}. Figure 13 shows data for two experiments where ozone decay was observed. The solar simulator was turned off after the ozone concentration reached a steady state value of 120 pphm. The mechanism used to compute the expected decay curve consists of reactions II, IV, and either D_1 or D_2. The value of k_{D_1} or k_{D_2} was found to completely control the ozone decay curve. The two curves in Fig. 13 show the best results obtained using either reaction D_1 or D_2. The values obtained are $k_{D_1} = 4\times10^{-4}$ sec^{-1} and $k_{D_2} = 5\times10^{6}$ cm^3/mole-sec. The curve using reaction D_1 (unimolecular decomposition) follows the trend of the experimental data somewhat better than the curve using the bimolecular destruction, reaction D_2.

The ozone destruction mechanism may not be exactly the same with the light on as with it off. Therefore, both reactions D_1 and D_2 were used (separately) in two series of computations to match the ozone formation experimental results. The value of k_{D_1} or k_{D_2} was first set at the value given above. Then the oxygen photolysis rate constant J_1 was changed to obtain good agreement between experimental and computed results for the beginning of the reaction. The k_{D_1} or k_{D_2} value was then varied slightly to match the experimental data for the end of the reaction. Figure 14 shows the results of these trials. The data points are for three different ozone formation experiments performed over a 2-month period before the chamber surface was exposed to any pollutant. The two curves are the computed curves obtained using the two different destruction reactions, D_1 and D_2. Rate constants used for these computations are $J_1 = 1\times10^{-9}$ sec^{-1}, $k_{D_1} = 3\times10^{-4}$ sec^{-1}, and $k_{D_2} = 4\times10^{6}$ cm^3/mole-sec. The two curves are very much the same. Either reproduces the experimental data quite well. These computations do not distinguish whether a first or second order O_3 destruction reaction occurs in the reaction chamber. Therefore, for the computations in the presence of pollutants, both reactions were considered. All computations were performed first using reaction D_1 and then repeated using reaction D_2. The rate constants used for all reactions considered in this work are listed in Table I.

Results With Nitric Oxide

Computations were performed for the case of nitric oxide added to dry air. The first mechanism used consists of reactions I through XI plus reaction D_2. The computed results did not agree qualitatively or quantitatively with the experimental results. The ozone concentration leveled off at a value much lower than that observed experimentally. No rate variations within estimated uncertainties changed these qualitative results. Adding two additional reactions, however, had a significant

effect on the computed ozone profile. These reactions, which involve nitrogen pentoxide, N_2O_5, are

$$NO_2 + NO_3 + M \xrightarrow{k_{22}} N_2O_5 + M \qquad \text{(XXII)}$$

$$h\nu + N_2O_5 \xrightarrow{J_{23a}} 2NO_2 + O \qquad \text{(XXIIIa)}$$

$$\xrightarrow{J_{23b}} NO_2 + NO_3 \qquad \text{(XXIIIb)}$$

A comparison of computed and experimental results using reactions XXII and XXIIIa is shown in Fig. 15(a) and (b). Part (a) shows computations using destruction reaction D_1 and part (b) shows computations using reaction D_2. For either reaction, the computed curves follow the qualitative trends of the experimental curves. For 30 pphm of NO, the computed delay in O_3 formation is longer than the observed delay. For the higher initial NO concentrations, the computed delay is shorter than that observed.

Analysis of the rates of formation and destruction of ozone by individual reactions shows that different ones are important at different times. At the beginning of the reaction the O_3 formed by reaction II is destroyed primarily by the reaction

$$NO + O_3 \rightarrow NO_2 + O_2 \qquad \text{(V)}$$

As ozone is built up it is also destroyed by

$$h\nu + O_3 \rightarrow O + O_2 \qquad \text{(III)}$$

Another destruction reaction that is relatively unimportant compared to the previous two reactions is

$$NO_2 + O_3 \rightarrow NO_3 + O_2 \qquad \text{(VIII)}$$

The additional destruction reactions D_1 and D_2 are even less important than reaction VIII in destroying O_3 at the start of the reaction.

At the end of the reaction, O_3 concentration levels off because reaction II is balanced primarily by the effect of the photolysis destruction, reaction III. The destruction reaction D_1 or D_2 has a much smaller effect in determining the final O_3 level for this system than for the pure air system. These computations support the previous interpretation of the experimental results. It was stated previously that the experimental results should be representative of homogeneous gas phase reaction in the chamber. The effect of the chamber walls is small during most of the reaction time.

Figure 16 shows several computed species concentration histories for the air + 65 pphm nitric oxide case. Comparison with the experimental curves shown in Fig. 6 indicates good qualitative agreement in general. Nitric oxide is rapidly converted to NO_2. Nitrogen dioxide concentration peaks at about the maximum slope of the ozone concentration curve, and then decreases. The experimental decrease of NO_2 (Fig. 6) is slower than that computed because the NO_2 measurement probably includes higher oxides of nitrogen. Computations show that N_2O_5 is formed slowly after about 20 minutes and increases to a steady-state value.

The preceding discussion refers to computations using reaction XXIIIa, the N_2O_5 photolysis reaction giving the products $2NO_2 + O$. All results are essentially the same when the computations are repeated using reaction XXIIIb, which gives the products $NO_2 + NO_3$. The computed concentration profiles were compared with those of the early computations, without any N_2O_5 reactions present. It was observed that NO_2 concentration remains high during most of the reaction when it cannot react to form N_2O_5. If NO_2 concentration stays high, computations show that it will destroy O_3 by the direct $NO_2 + O_3$ reaction. The present analysis gives no information about the products of the N_2O_5 photolysis.

Results With NO, CO, and H_2O

The mechanism for O_3 chemistry in the presence of CO, NO, and H_2O includes reactions I to XXIII plus reactions which provide OH radicals. The latter are necessary for starting the chain (reactions XII to XV) which converts NO to NO_2 without the destruction of O_3. The following photolysis reactions were used as the source for OH:

$$h\nu + H_2O \xrightarrow{J_{24}} OH + H \qquad \text{(XXIV)}$$

$$h\nu + H_2O_2 \xrightarrow{J_{25}} OH + OH \qquad \text{(XXV)}$$

$$h\nu + HNO_2 \xrightarrow{J_{26}} NO + OH \qquad \text{(XXVI)}$$

$$h\nu + HO_2 \xrightarrow{J_{27}} O + OH \qquad \text{(XXVII)}$$

Hydrogen peroxide, H_2O_2, is formed by the reaction

$$HO_2 + HO_2 \xrightarrow{k_{28}} H_2O_2 + O_2 \qquad \text{(XXVIII)}$$

Rate constants for the photolysis reactions were chosen to give satisfactory agreement with the experimental results. The values used are generally within a factor of 4 of those given by McConnell and McElroy (1973) for an altitude of 80 km. However, J_{24}, the H_2O photolysis rate constant, was taken as 1/10th of their value. Computations show that the two important sources of OH in our mechanism are the H_2O and H_2O_2 photolyses.

The rate constants used in the dry air plus NO computations were not changed for the computations with CO and H_2O also present. Computed results were found to be only slightly different using O_3 destruction

reaction D_1 from results using reaction D_2. Inasmuch as the 10 percent higher final O_3 concentration using D_2 was more in agreement with experiment, the computations to be discussed use reaction D_2.

Figure 17 shows both the experimental and typical computed results for O_3 production in air containing 50 ppm CO, 75 pphm NO, and 1200 ppm H_2O. Also shown for comparison are experimental and computed O_3 concentration curves for "UPC" air + 65 pphm NO added initially. These last two curves are the same ones shown in Fig. 15(b). There is poor quantitative agreement between experimental and computed curves in the presence of CO and H_2O. However, the computed results show the same qualitative effect of CO that is observed experimentally. The computed delay in O_3 formation is much less in the presence of CO and H_2O. It is clear that the computations do not fully explain the chemical reaction in the presence of CO and H_2O. The slope of the main portion of the computed curve is much lower than that for the experimental curve. Moreover, the steady state O_3 concentration is also lower on the computed curve. Another problem is the failure of the computations to show increased effectiveness of higher CO initial concentrations. The computed results for 200 ppm CO present show a significantly smaller difference from the results for 50 ppm CO than is observed experimentally. The qualitative trend is shown, but there is no quantitative agreement. Many rate constant variations showed that the actual delay in O_3 formation is quite sensitive to the rate constants J_{24} and J_{25} for photochemical formation of OH radical. However, for all perturbations of other rate constants within their estimated uncertainty, the slope of the main portion of the O_3 concentration curve and the final O_3 level were changed only slightly.

One final point concerning the reactions of NO_2 formed from the original NO, should be mentioned. We have discussed earlier the possibility of the removal of higher oxides of nitrogen from the gas phase as HNO_3 condensed on the chamber walls (Gay and Bufalini (1971)). This idea provides one possible reason for the disagreement between computed and experimental O_3 production. The computations do not allow the removal of higher oxides of nitrogen from the gas phase.

Our reaction mechanism gives only a relatively small amount of indirect conversion of N_2O_5 to HNO_3 via reactions XXIII and XX. This is certainly unrealistic. Our gas phase mechanism does not properly explain the subsequent reactions of NO_2. Additional computations must be done to better explain our experimental results.

CONCLUDING REMARKS

The main concern about the effect of nitric oxide emission in the stratosphere has been its possible long lasting destruction of ozone. Many papers (e.g., Johnston (1971), Westenberg (1972)) have predicted that NO destroys ozone catalytically, i.e., without itself being destroyed. These conclusions were based on approximate steady state analyses and the assumption that all the NO_2 formed by reaction V would be photolyzed back to NO by reaction VI. The present laboratory scale experiment indicates that NO is destroyed while destroying O_3. The O_3 formation reaches its usual level (in the absence of pollutants) soon after most of the NO has been converted to NO_2 and other oxides of nitrogen. Even though NO_2 is partially photolyzed back to NO, this reaction also produces oxygen atoms. These, along with the O atoms from the photolysis of O_2, form more ozone than the regenerated NO can destroy. The computations for dry air with NO added show that NO is destroyed much faster by the NO + O_3 reaction than it is regenerated by NO_2 photolysis in the early stages of the reaction. In the latter part of the reaction NO concentration becomes quite low. Then the NO concentration stays at this low level because its formation by NO_2 photolysis (and the reaction $O + NO_2 \rightarrow NO + O_2$) is exactly balanced by its destruction in the $NO + O_3$ reaction. At this time the O_3 forming reactions cause the O_3 level to build up to its usual level in the absence of NO.

The effect of CO and H_2O, which increases O_3 concentration in the present experiment, is not completely understood. Since these products are present, along with NO, in engine exhausts, the matter of equilibrium O_3 concentration in the presence of engine discharges is still uncertain.

An important question is whether our laboratory results can be applied to low pressure conditions. To partly answer this question, the experiments and the theoretical computations just described will be repeated at reduced pressures, down to about 0.3 atm. The latter pressure is the expected lower limit, based on preliminary tests of our modified O_3 analyzer. If the theoretical modelling is successful at this reduced pressure, the same chemical mechanism will be used for theoretical computations at stratospheric pressures. The attempt will be made to predict the trend of O_3 formation in the presence of pollutants down to 0.05 atm. The ratios of the various pollutants will be adjusted to simulate upper atmospheric concentrations.

REFERENCES

Baulch, D. L., D. D. Drysdale and A. C. Lloyd, 1969: High Temperature Reaction Rate Data. Rept. 3, Dept. Phys. Chem., Leeds Univ.

Bittker, D. A., and V. J. Scullin, 1972: General Chemical Kinetics Computer Program for Static and Flow Reactions, With Application to Combustion and Shock-Tube Kinetics. NASA Tech. Note D-6586, 187 pp.

Crutzen, P. J., 1972: The Photochemistry of the Stratosphere with Special Attention Given to the Effects of NO_x Emitted by Supersonic Aircraft. Proc. Survey Conf. on Climatic Impact Assessment Program, Feb. 15-16, pp. 80-89.

Davis, D. D., 1972: Recent Kinetic Measurements on Reactions of $O(^3P)$, H and HO_2. Proc. Sec. Conf. on Climatic Impact Assessment Program. Nov. 14-17, pp. 126-143.

DeMore, W. B., 1973: Rate Constants for Reactions of Hydroxyl and Hydroperoxyl Radicals with Ozone. Sci., 180, pp. 735-737.

Dütsch, H. U., 1972: The Present Status of Ozone Research: Photochemistry and Observations. Proc. Sec. Conf. on Climatic Impact Assessment Program, Nov. 14-17, pp. 106-113.

Garvin, D., ed., 1973: Chemical Kinetics Data Survey V. Sixty-six Contributed Rate and Photochemical Data Evaluations on Ninety-Four Reactions. Rept. NBSIR 73-206, National Bureau of Standards.

Garvin, D. and R. F. Hampson, eds., 1974: Chemical Kinetics Data Survey VII. Tables of Rate and Photochemical Data for Modelling of the Stratosphere (Revised). Rept. NBSIR 74-430, National Bureau of Standards.

Gay, B. W., Jr., and J. J. Bufalini, 1971: Nitric Acid and the Nitrogen Balance of Irradiated Hydrocarbons in the Presence of Oxides of Nitrogen. Env. Sci. Techn., 5, pp. 422-425.

Hampson, R. F., ed., 1972: Chemical Kinetics Data Survey I. Rate Data for Twelve Reactions of Interest for Stratospheric Chemistry. Rept. 10 692, National Bureau of Standards.

Heicklen, J., K. Westberg and N. Cohen, 1969: Conversion of NO to NO_2 in Polluted Atmospheres. Chemical Reactions in Urban Atmospheres. American Elsevier Pub. Co., pp. 55-58.

Johnston, H. S., 1971: Reduction of Stratospheric Ozone by Nitrogen Oxide Catalysis for Supersonic Transport Exhaust. Sci., 173, pp. 517-22.

Kellogg, W. W., chairman, Work Group on Climatic Effects, 1970: Man's Impact on the Global Environment: Report of the Study of Critical Environmental Problems, M.I.T. Press, pp. 100-112.

Leighton, Philip A., 1961: Photochemistry of Air Pollution. Academic Press.

McConnell, J. C., and M. B. McElroy, 1973: Odd Nitrogen in the Atmosphere. J. Atm. Sci., 30, pp. 1465-80.

Simonaitis, R. and J. Heicklen, 1972: The Reaction of OH With NO_2 and Deactivation of $O(^1D)$ by CO. Int. J. Chem. Kinetics, 4, pp. 529-40.

Schofield, K., 1967: An Evaluation of Kinetic Rate Data for Reactions of Neutrals of Atmospheric Interest. Planet. Space Sci. 15, pp. 643-70.

Westberg, K. and N. Cohen, 1971: Carbon Monoxide: Its Role in Photochemical Smog. Sci., 171, pp. 1013-1015.

Westenberg, A. A., 1972: Effect of NO_x on Stratospheric Ozone. Tech. Memo. TG 1186, Johns Hopkins Univ. Applied Physics Laboratory.

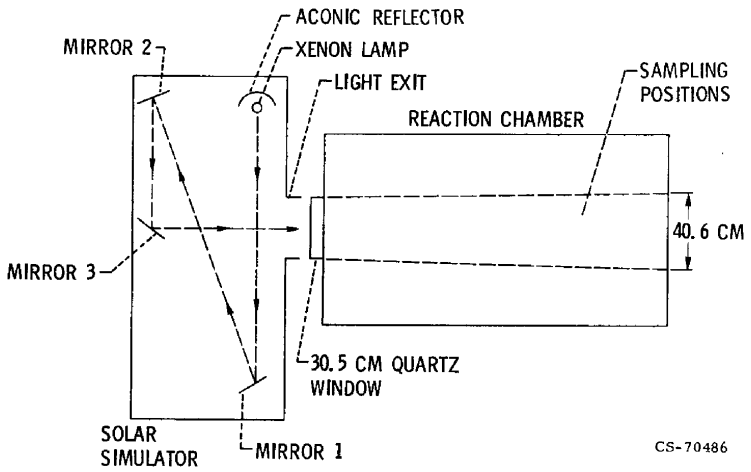

Figure 1. - Simulator and reaction chamber.

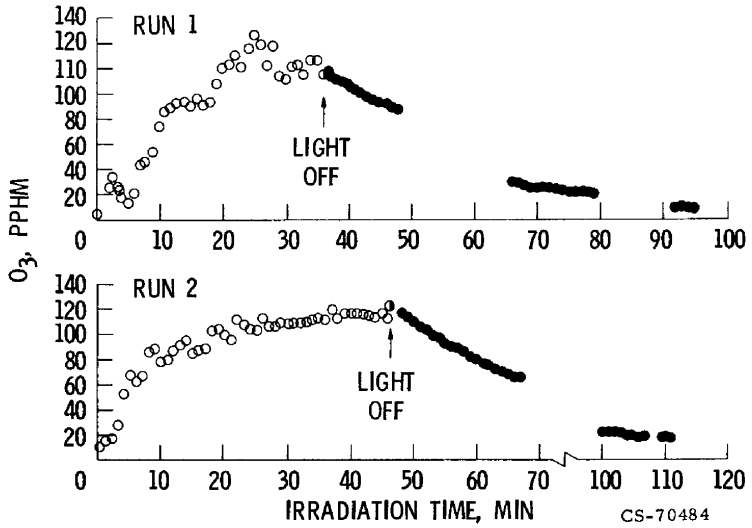

Figure 2. - Ozone production for "UPC" air.

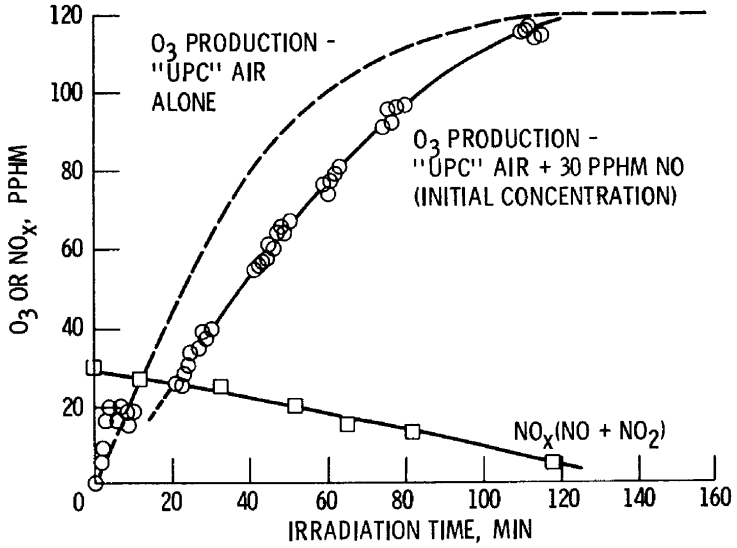

Figure 3. - Ozone production for "UPC" air containing 30 pphm NO.

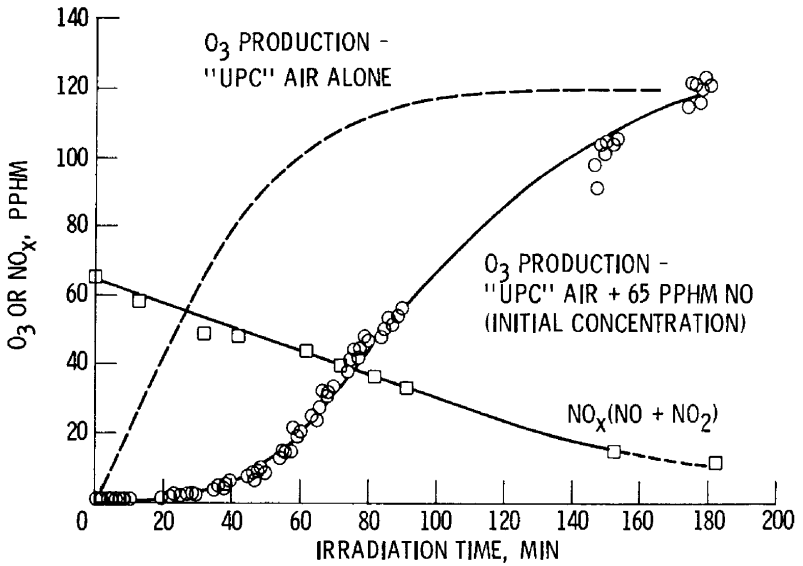

Figure 4. - Ozone production for "UPC" air containing 65 pphm NO.

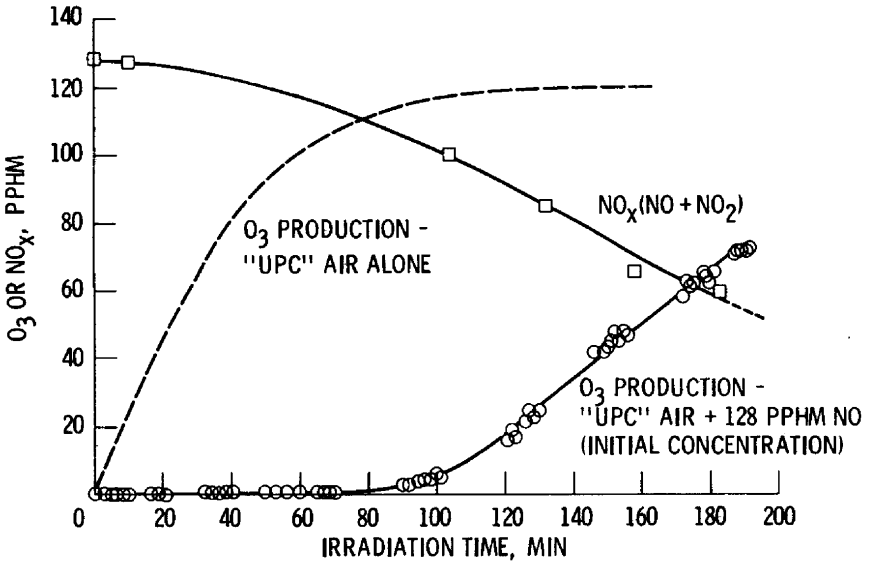

Figure 5. - Ozone production for "UPC" air containing 128 pphm NO.

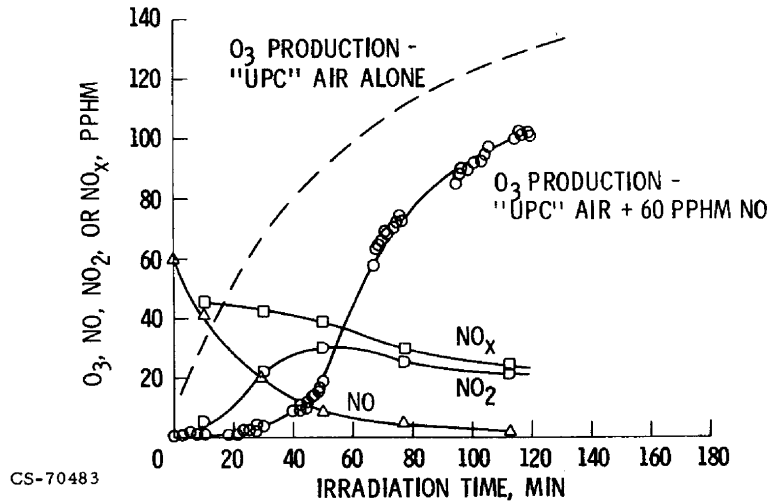

Figure 6. - O_3 production for "UPC" air containing 60 pphm NO.

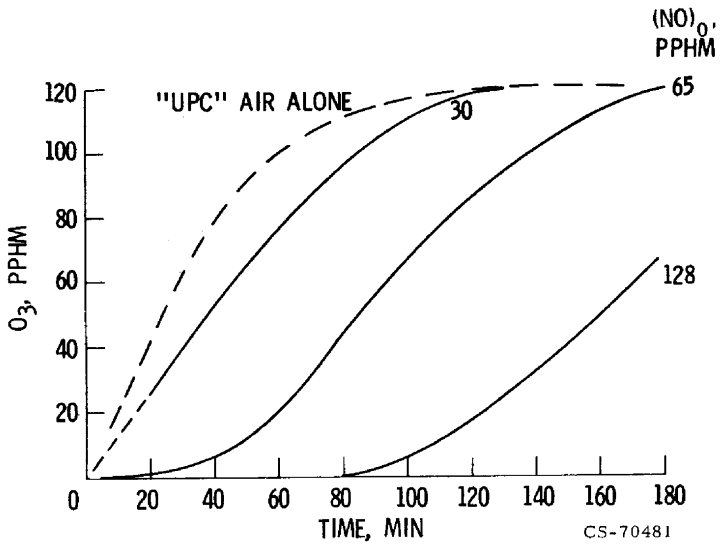

Figure 7. - O_3 production for "UPC" air containing various initial amounts of NO.

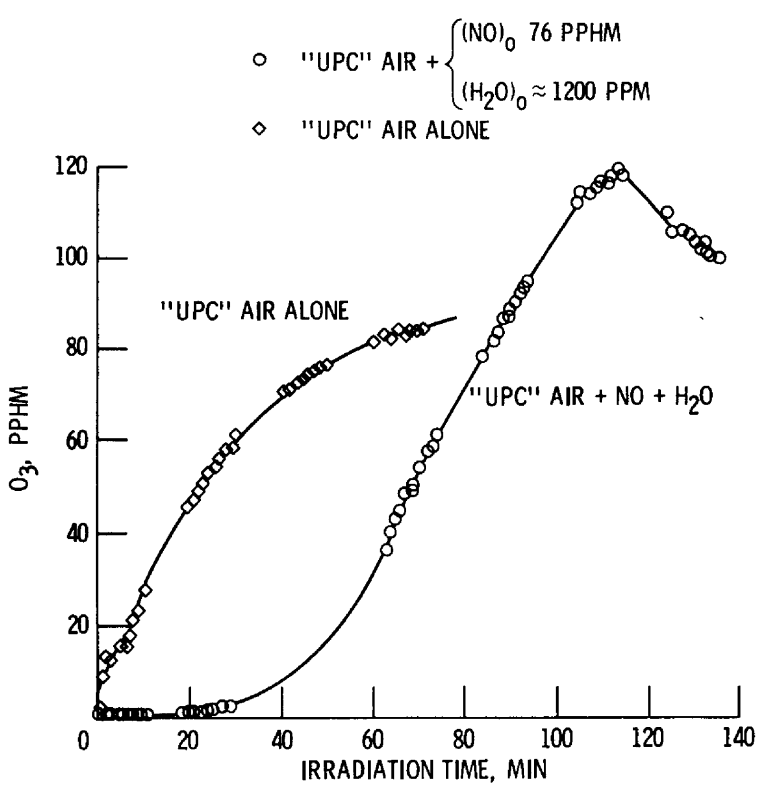

Figure 8. - Ozone production for "UPC" air containing 76 pphm NO and 1200 ppm H_2O.

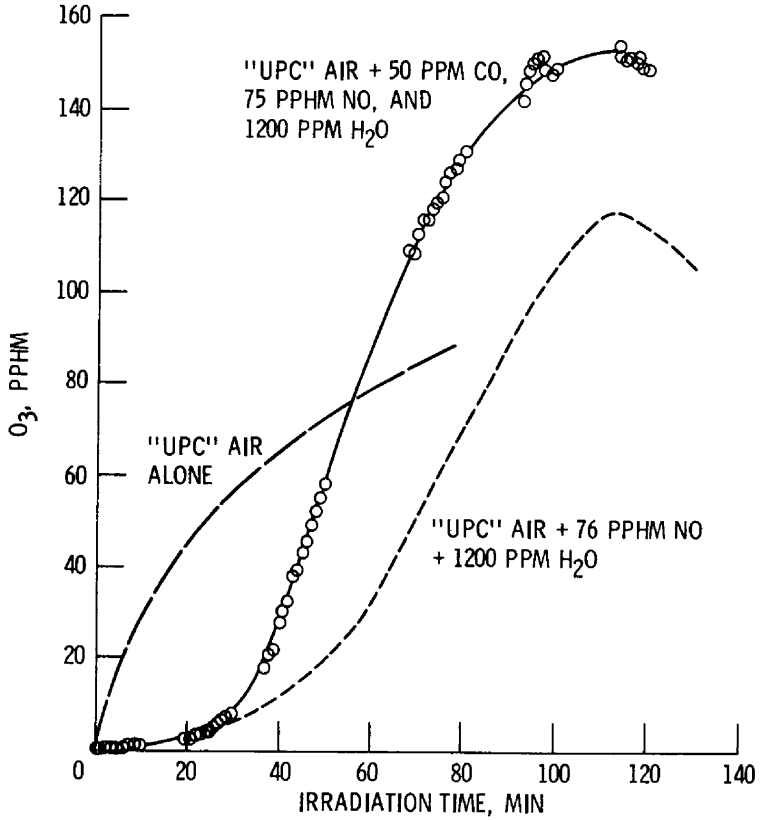

Figure 9. - Ozone production for "UPC" air containing about 50 ppm CO, 75 pphm NO, and 1200 ppm H_2O.

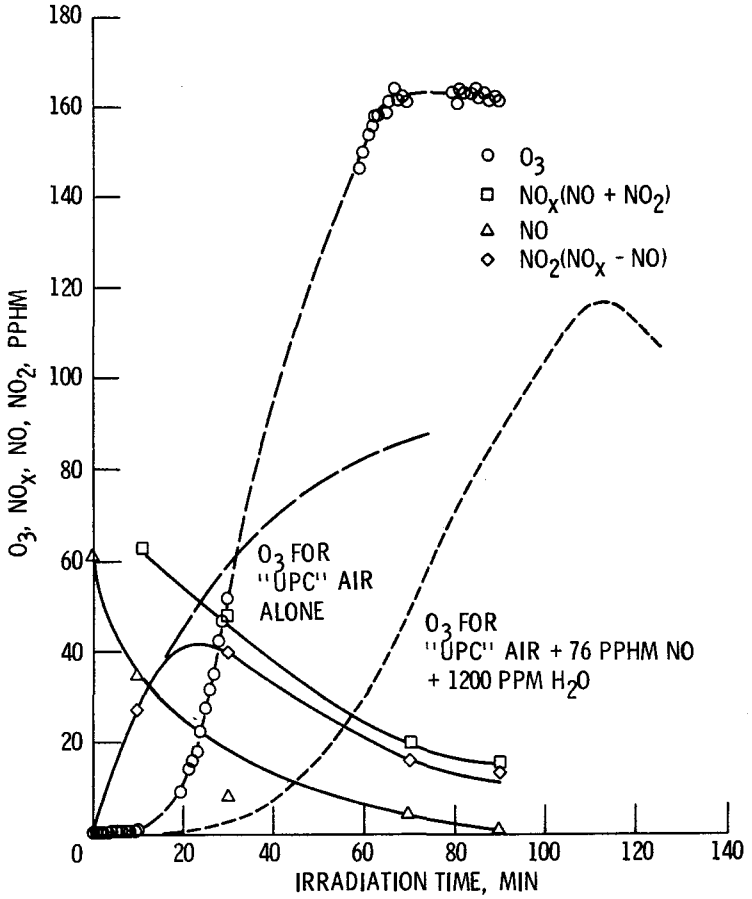

Figure 10. - Ozone production for "UPC" air containing about 100 ppm CO, 60 pphm NO, and 1200 ppm H_2O.

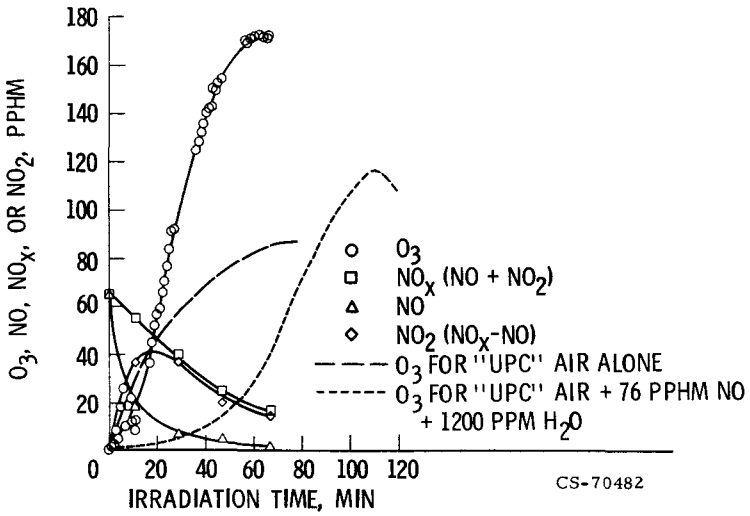

Figure 11. - Ozone production for "UPC" air containing about 220 ppm CO, 65 pphm NO, and 1200 ppm H_2O.

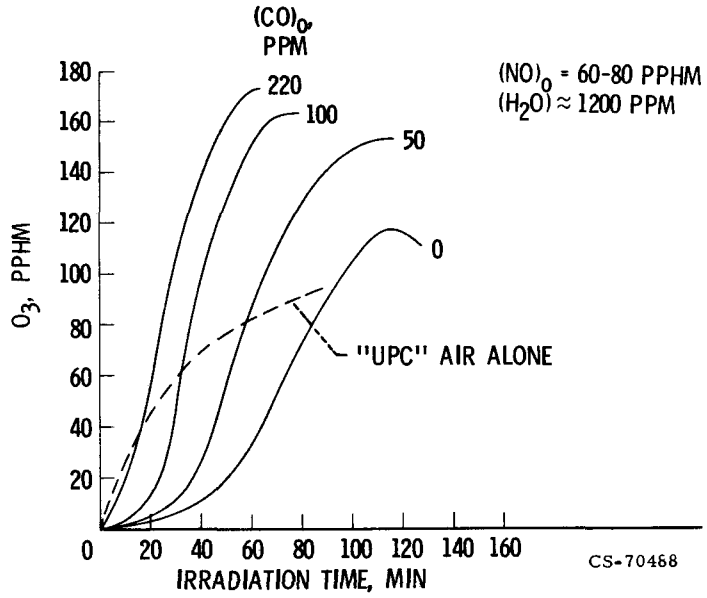

Figure 12. - Ozone production when various amounts of CO are added to "UPC" air containing some NO and H_2O.

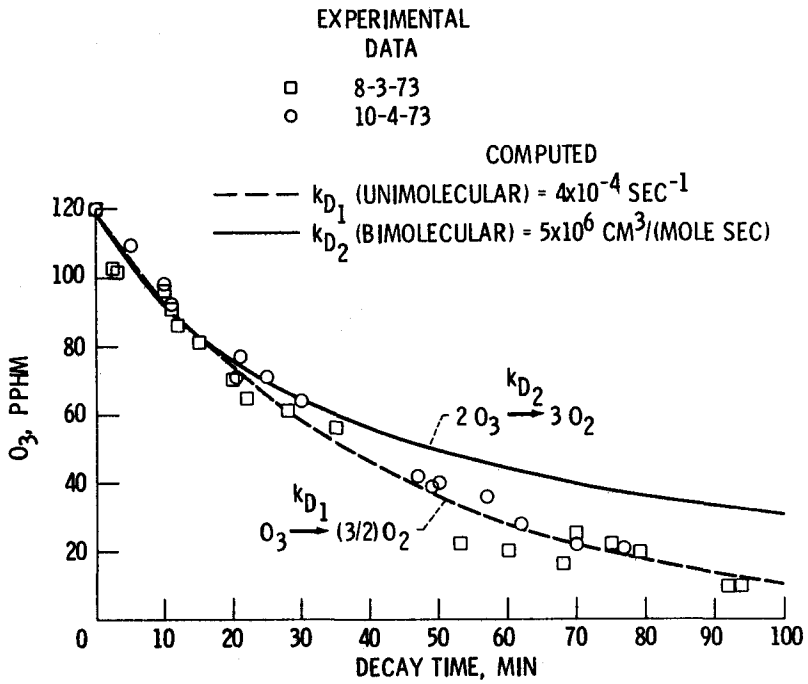

Figure 13. - Ozone destruction in "UPC" air; experimental and theoretical.

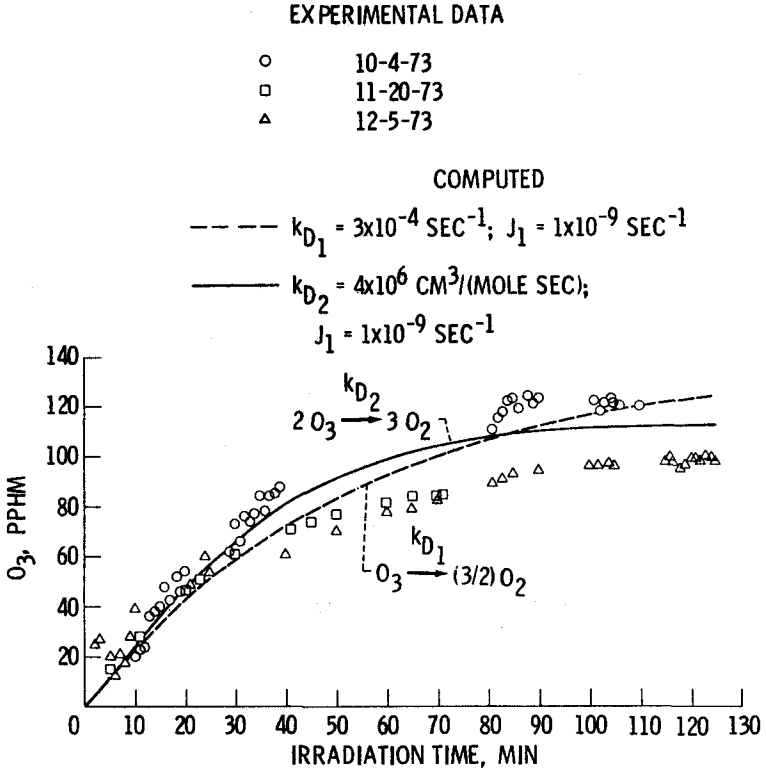

Figure 14. - Ozone formation in "UPC" air; experimental and theoretical.

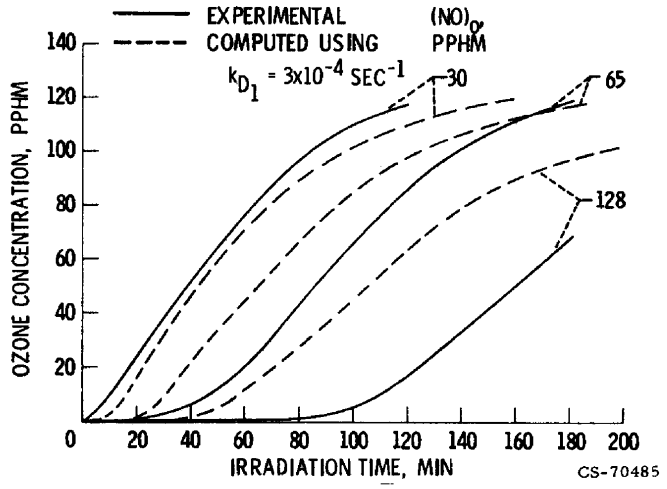

(a) USING $O_3 \xrightarrow{k_{D_1}} (3/2)O_2$.

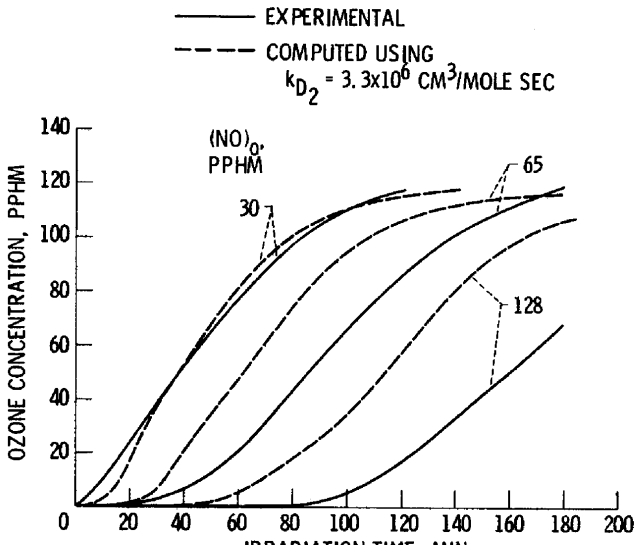

(b) USING $2\,O_3 \xrightarrow{k_{D_2}} 3\,O_2$.

Figure 15. - Comparison of experimental and theoretical ozone formation in air + nitric oxide mixtures.

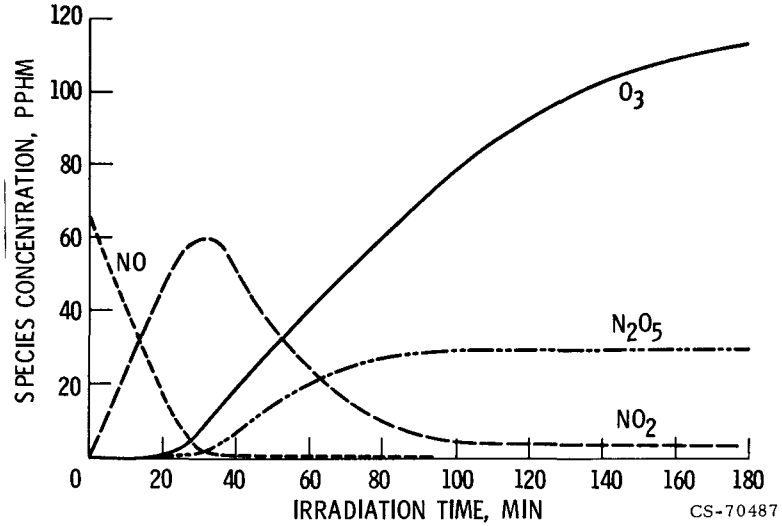

Figure 16. - Species concentration vs. time for irradiation of air + 65 pphm nitric oxide; computed results using unimolecular destruction reaction, $O_3 \rightarrow (3/2)O_2$.

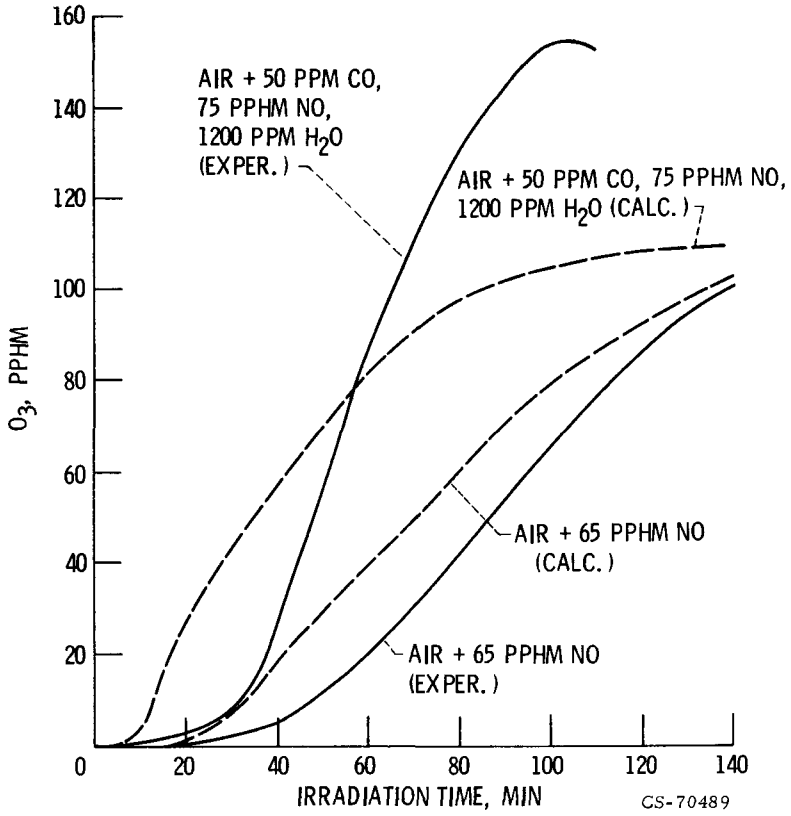

Figure 17. - Effect of CO, NO, and H_2O on O_3 formation.

NASA-Lewis

TABLE I. - CHEMICAL REACTIONS AND RATE CONSTANTS

Number	Reaction	Preexponential factor,* A	Temperature exponent,* n	Activation energy,* kcal/mole	References
I	$h\nu + O_2 \rightarrow O + O$	1×10^{-9}	0.0	0.0	See text
II	$O + O_2 + M \rightarrow O_3 + M$	3.83×10^{13}		-1.01	Garvin and Hampson (1974) M = N_2
III	$h\nu + O_3 \rightarrow O + O_2$	3.55×10^{-3}		.0	Westenberg (1972)†
IV	$O + O_3 \rightarrow O_2 + O_2$	1.1×10^{13}		4.57	Garvin and Hampson (1974)
V	$NO + O_3 \rightarrow NO_2 + O_2$	5.5×10^{11}		2.39	Garvin and Hampson (1974)
VI	$h\nu + NO_2 \rightarrow NO + O$	1×10^{-3}		.0	McConnell and McElroy (1973)†
VII	$O + NO_2 \rightarrow NO + O_2$	5.5×10^{12}		.0	Garvin and Hampson (1974)**
VIII	$NO_2 + O_3 \rightarrow NO_3 + O_2$	3×10^{7}		.0	Garvin and Hampson (1974)**
IX	$2NO + O_2 \rightarrow 2NO_2$	1.2×10^{9}		-1.05	Garvin and Hampson (1974)
X	$NO + O + M \rightarrow NO_2 + M$	9.4×10^{14}		-1.93	Schofield (1967)
XI	$h\nu + NO_3 \rightarrow NO + O_2$	1×10^{-3}		.0	McConnell and McElroy (1973)†
XII	$CO + OH \rightarrow CO_2 + H$	8.7×10^{10}		.0	Garvin and Hampson (1974)**
XIII	$H + O_2 + M \rightarrow HO_2 + M$	1.59×10^{15}		-1.0	Baulch, et al. (1969) M = Ar‡
XIV	$NO + HO_2 \rightarrow NO_2 + OH$	3.6×10^{11}		.0	Davis (1972)†,**
XV	$H + NO_2 \rightarrow NO + OH$	2.9×10^{13}		.0	Garvin and Hampson (1974)**
XVI	$OH + O_3 \rightarrow HO_2 + O_2$	3×10^{11}		1.99	Garvin and Hampson (1974)†
XVII	$HO_2 + O_3 \rightarrow OH + 2O_2$	3×10^{10}		2.49	Garvin and Hampson (1974)†
XVIII	$NO + OH + M \rightarrow HNO_2 + M$	3×10^{16}		.0	Garvin and Hampson (1974)**
XIX	$OH + HNO_2 \rightarrow H_2O + NO_2$	8.4×10^{11}		1.99	Hampson (1972)
XX	$NO_2 + OH + M \rightarrow HNO_3 + M$	8×10^{16}		.0	Simonaitis and Heicklen (1972)**
XXI	$OH + HNO_3 \rightarrow H_2O + NO_3$	8.4×10^{11}		1.99	Hampson (1972)
XXII	$NO_2 + NO_3 + M \rightarrow N_2O_5 + M$	1×10^{18}		.0	Garvin (1973)**
XXIIIa	$h\nu + N_2O_5 \rightarrow 2NO_2 + O$	1×10^{-4}		.0	Johnston (1971)†
XXIIIb	$h\nu + N_2O_5 \rightarrow NO_2 + NO_3$	7.7×10^{-5}		.0	McConnell and McElroy (1973)
XXIV	$h\nu + H_2O \rightarrow H + OH$	1×10^{-7}		.0	McConnell and McElroy (1973)†
XXV	$h\nu + H_2O_2 \rightarrow OH + OH$	5.7×10^{-5}		.0	McConnell and McElroy (1973)
XXVI	$h\nu + HNO_2 \rightarrow NO + OH$	1.3×10^{-3}		.0	McConnell and McElroy (1973)
XXVII	$h\nu + HO_2 \rightarrow O + OH$	3.9×10^{-4}		.0	McConnell and McElroy (1973)
XXVIII	$HO_2 + HO_2 \rightarrow H_2O_2 + O_2$	5×10^{12}		.99	Garvin and Hampson (1974)†

*Constants in the equation $k = AT^n \exp(-E_a/RT)$. Units of k are sec^{-1} for photochemical reaction, cm^3/mole sec for bimolecular reaction; and cm^6/mole^2 sec for termolecular reaction.

†Adjusted from value given in reference.

‡Third body relative efficiencies, N_2/Ar and O_2/Ar, for this reaction are taken as 2. A more recent recommended equation (Garvin and Hampson (1974)) gives a value about 20 percent lower at T = 300 K.

**Temperature = 298 K.